EasyChair Preprint

№ 7425

CMOS-Based Biosensor Using Broadband Tunable Active-Inductor-Based VCO with γ-Dispersion for Detecting CTCs and Exosomes

Takuya Tsujimura, Shunya Murakami, Guowei Chen,
Yuma Hayashi, Sora Kato, Akiyoshi Tanaka and Kiichi Niitsu

February 7, 2022

CMOS-Based Biosensor Using Broadband Tunable Active-Inductor-Based VCO with γ-Dispersion for Detecting CTCs and Exosomes

Takuya Tsujimura[1], Shunya Murakami[1], Guowei Chen[1], Yuma Hayashi[1],
Sora Kato[1], Shinichi ito[1], Akiyoshi Tanaka[1], and Kiichi Niitsu[1,2]
[1]Nagoya University, Japan,
[2]JST/PRESTO, Saitama, Japan
Email: tsujimura.takuya@j.mbox.nagoya-u.ac.jp, niitsu@nuee.nagoya-u.ac.jp

***Abstract*—In this paper, we propose a CMOS biosensor that can be extensively tuned by voltage control using an active inductor. In order to detect circulating tumor cells (CTCs) and exosomes, a voltage-controlled oscillator (VCO) with active inductors is employed to operate at a wider frequency range with a chip area of 0.086 mm^2 including PAD, which is smaller than that of conventional circuits. To verify the operation of the proposed biosensor, electromagnetic (EM) simulation shows that the electric field extends to the cells on the interdigital capacitor (IDC) in the sensing area. Based on the simulation results, we conducted experiments on a prototype fabricated using the TSMC 65-nm standard process. The biosensor was found to vary from about 1.78-4.43 GHz with a power consumption of 39.0-45.8 mW. 2 µl of purified water was dropped onto the sensor multiple times and successfully detected water with an average frequency shift of 0.702 GHz. These results indicate that the proposed biosensor has the potential to detect biomarkers such as CTCs and exosomes.**

Keywords—CMOS, biosensors, active inductor, circulating tumor cells (CTCs), exosomes, interdigital capacitor (IDC).

I. Introduction

In recent years, biomarkers such as circulating tumor cells (CTCs) and exosomes have been attracting attention for the early detection and treatment of cancer. There are several biological substances that have attracted attention as biomarkers in liquid biopsy, and Circulating Tumor cells (CTCs) and exosomes, which are extracellular vesicles containing genetic information such as mRNA, are representative examples. By detecting these biomarkers in body fluids and analyzing the genetic information contained in them, highly accurate and label-free cancer diagnosis based on the genetic information of cells is possible, and minimally invasive cancer treatment can be realized [1], [2].

Currently, the main biosensors are based on optical methods. The optical method requires label processing and is expected to have various applications with high sensitivity, but it has the disadvantage of large size and high cost because it requires equipment such as a light source, spectrometer, and detector. Therefore, optical methods limit the possibility of developing simple inspection methods [3]. On the other hand, electrical methods, such as those represented by CMOS biosensor integrated circuits, do not require label processing, and have the advantage of simple and rapid detection with small equipment, as well as low cost due to mass production of integrated circuit chips. Therefore, the electrical method using dielectric properties has the potential to realize a simple and inexpensive device for liquid biopsy using CTCs and exosomes as biomarkers.

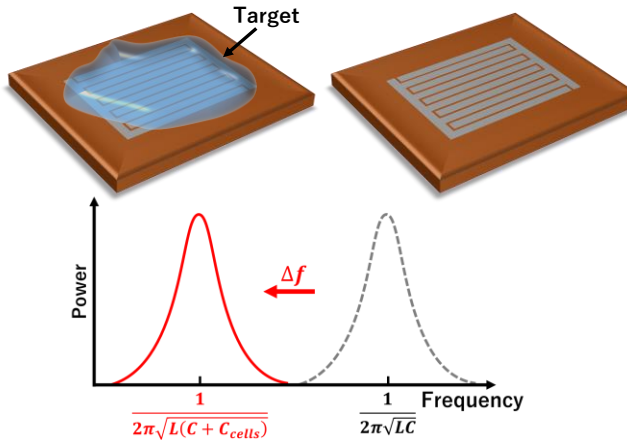

Fig. 1. Conceptual image of the proposed biosensor.

In previous studies, several biosensors have been proposed based on the frequency shift of LC oscillators [4]-[6]. The disadvantage of these sensors is that their operation is narrow-banded due to the use of LC oscillators. In this study, we confirmed by EM simulation that the electric field extends over the chip, and verified the effectiveness of the proposed biosensor from actual measurements of water drops on the prototype sensor.

II. System of Proposed Biosensor

Fig. 1 shows the conceptual diagram of our proposed biosensor. The target biological material is detected by using the frequency change of the LC oscillator to detect it. The operating frequency of the LC oscillator is expressed as follows:

$$f = \frac{1}{2\pi\sqrt{LC}} \quad (1)$$

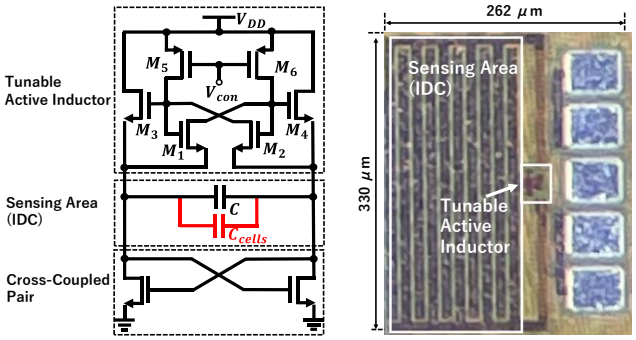

(a) (b)

Fig. 2. Schematic of biosensing system.

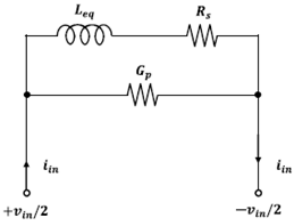

Fig. 3. Small-signal equivalent circuit of a simplified active inductor.

where L and C represent inductance and capacitance, respectively. The value of capacitance increases with the dielectric constant of biomarkers such as CTCs and exosomes placed on the biosensor chip. If the value of capacitance increased by cells is C_{cells}, the new oscillation frequency can be rewritten as follows:

$$f = \frac{1}{2\pi\sqrt{L(C + C_{cells})}}. \tag{2}$$

Based on the change in this oscillation frequency, biomarkers can be detected. In this LC-oscillator-based sensor, target molecules can be detected even when the target and the circuit are far apart. In determining the operating frequency, we focused on the dielectric dispersion of biological tissues and cells.

Due to polarization of counterions, interfacial polarization between cell membrane and cytoplasm, and dielectric dispersion of bound water, α-dispersion (-10 kHz), β-dispersion (1-100 MHz), and γ-dispersion (1 GHz-) occur in cells, respectively [7], [8]. Since the relaxation of bound water can be observed in the GHz band, cells can be detected, and we aim to realize a broadband VCO to directly capture the dielectric relaxation caused by the intercellular structure.

Fig. 2 shows the proposed biosensor. The circuit consists of a variable active inductor, a sensing region, and a cross-coupled pair, where the inductance can be varied with voltage V_{con} [9]. The designed circuit area is 0.086 mm^2 . For the active inductor, if only the DC component is taken into account, transistors M_1 and M_2 form a cross-coupled pair, while M_3 and M_4 form a drain-grounded amplifier circuit. Also, at the operating point of the circuit, M_1, M_2, M_3, and M_4 are all in the saturation region. M_5 and M_6 are modeled by g_{ds5} and g_{ds6} at the operating point, respectively. When $2g_{m1}+g_{m3} > g_{ds5}$, the circuit shown in Fig. 3 can be simplified using the equivalent inductance L_{eq} ,

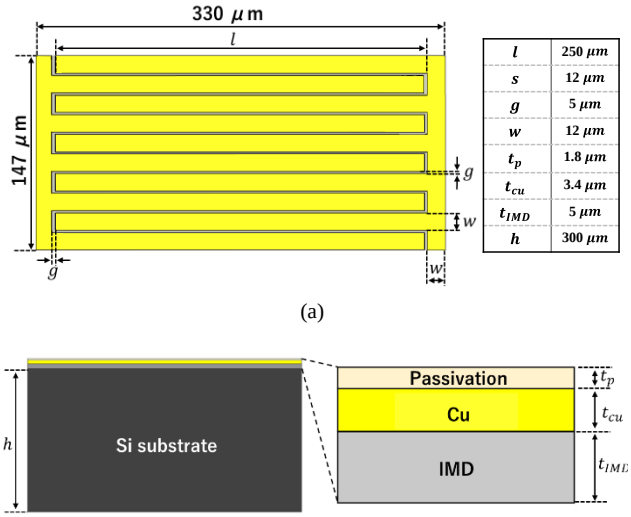

(a)

(b)

Fig. 4. Architecture of the designed IDC. (a) Top view, (b) Side view.

resistance R_S, and conductance G_p of the active inductor. Each parameter is shown as follows:

$$L_{eq} = \frac{2(C_{GS1} + C_{GS3})}{g_{ds5}(2g_{m1} + g_{m3} - g_{ds5})}, \tag{3}$$

$$R_s = \frac{2(g_{ds5} + g_{m1})}{g_{ds5}(2g_{m1} + g_{m3} - g_{ds5})}, \tag{4}$$

$$G_p = \frac{g_{ds5}}{2}. \tag{5}$$

III. Simulation Results

A. Electromagnetic simulation

Fig. 4 shows the designed IDC. For the capacitance of the sensing area, the interdigital capacitor (IDC) consists of multiple fingers and is a capacitor that utilizes the capacitance generated in the gap between conductors. When a standard capacitor is used, the electric field does not extend over the chip, but when an IDC is used, the electric field extends over the chip and the presence of a measurement target changes the equivalent capacitance value. Therefore, it can be used not only to detect the presence or absence of a target, but also to measure conductivity, permeability, and dielectric constant [10]. Since the proposed circuit is fabricated in the TSMC 65 nm CMOS process, the thickness and dielectric constant values of the passivation layer, copper interconnections, and internal dielectric layer were determined with reference to the process rule. Since the top metal in the CMOS process used to fabricate this circuit is the ninth layer, the internal dielectric (IMD) is stacked to correspond to the ninth metal layer. The design of this IDC has a capacitance of about 250 fF. The simulation was performed using CST Microwave Studio 2021 for electromagnetic field simulation to evaluate the electric field distribution of the IDC. Fig. 5 shows the electric field distribution when a differential signal is given to the designed

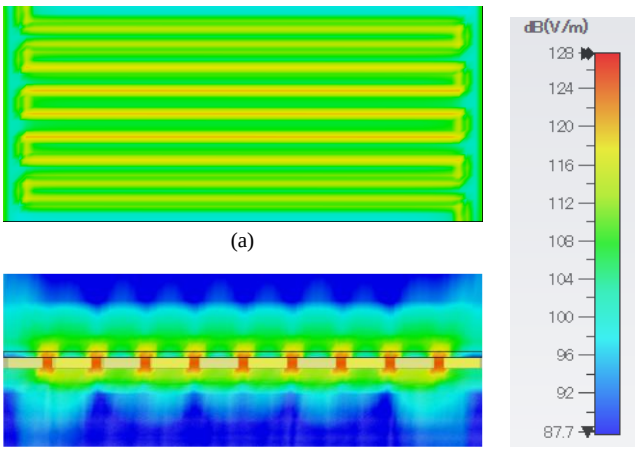

(a)

(b)

Fig. 5. Electromagnetic simulation of the designed IDC. (a) Top view, (b) Cross section.

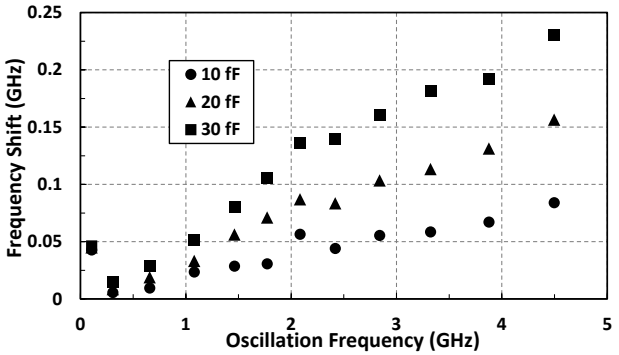

Fig. 6. Simulated relationsip between oscilllation frequency and frequency shift.

IDC. From the simulation results, it was determined that the electric field generated by the IDC would spread to the top of the passivation layer, and the electric field would be sufficiently applied to the target dropped on the chip.

B. Post layout simulation

In order to verify the feasibility of the proposed concept, simulations were performed using the Process Design Kit (PDK) for the TSMC 65-nm standard CMOS process, after extracting the wiring parasitic elements and the instance parameters of the specified design elements in the designed layout.

Since there is limited information on the dielectric properties of CTCs and exosomes, in this simulation, the equivalent capacitance of the cell (C_{cells} in Fig. 2(a)) was set to 10 fF, the value of capacitance of a typical cell, based on the dielectric parameters of a typical cell [11]. Furthermore, the simulation results of the relationship between the oscillation frequency and frequency shift when the capacitance to be added is changed to 20 fF and 30 fF are shown in Fig. 6. Since the magnitude of the frequency shift changes by changing the value of the added capacitance, it can be confirmed that the system is capable of detecting parameters that affect the dielectric properties of biomaterials, such as the size and concentration of biomaterials.

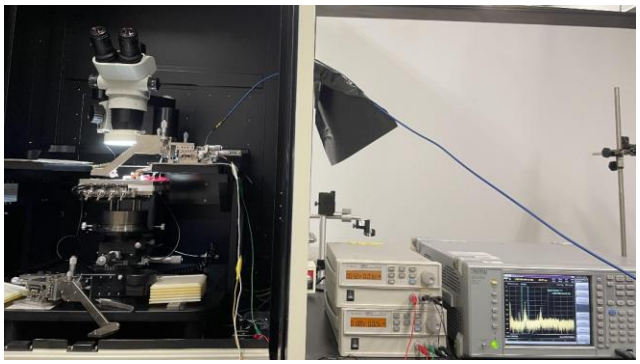

Fig. 7. Measurement setup.

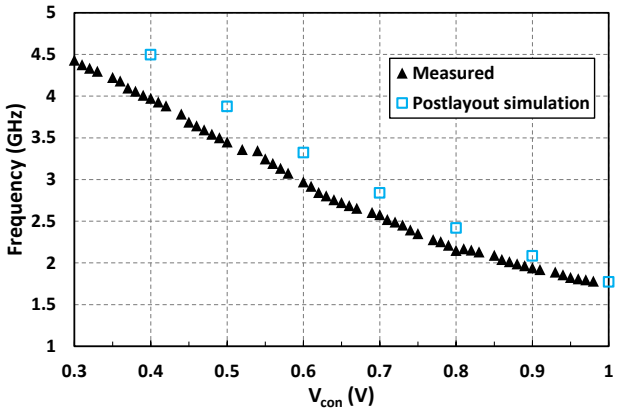

Fig. 8. Relationship between V_{con} and oscillation frequency. (The range of V_{con} is from 0.3 to 1.0 V.)

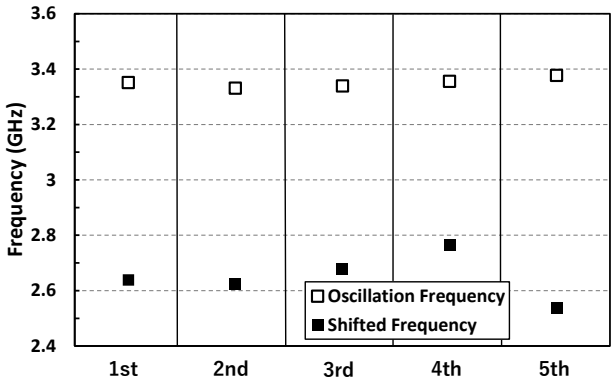

Fig. 9. Measured frequency shifts.

IV. MEASUREMENT RESULTS

The spectrum analyzer (Anritsu MS2830A) and the power supply (Agilent U8002A) have been used for the measurement. The output has been connected to the spectrum analyzer via SMA cables. The supply voltage other than V_{con} is 1.8 V. The post layout simulation and the actual measurement results of the prototype chip are shown in Fig. 8. The proposed biosensor achieves a wide frequency range of about 1.78-4.43 GHz depending on the V_{con}, and the oscillation frequency changes linearly depending on the V_{con}. In the postlayout simulation, the oscillation frequency only started at V_{con} of 0.4 V, but in the prototype chip, the oscillation frequency was the same at 0.3 V due to the influence of parasitic capacitance. The power consumption was 39.0-45.8 mW. The operating frequency and

TABLE I. COMPARISON TO THE PREVIOUS WORKS

	JSSC' 2016 [4]	JSSC' 2018 [5]	APCCAS' 2019 [6]	This Work
Circuit configuration	LC-VCO (Injection Locked)	LC-VCO (Transformer)	LC-VCO (Inductive)	LC-VCO (Active Inductor and IDC)
Operation frequency (GHz)	6.5/11/17/30 (4ch)	1.4/3.7	0.00113	1.78–4.43
Detection limit (ppm)	1.25	0.3	70	N.A.
Power consumption (mW)	65	5.0	39.6	39.0–45.8
Circuit Area (mm^2)	0.212	0.17	1.13	0.086
CMOS Technology	65 nm	65 nm	65 nm	65 nm
Label	Unnecessary	Magnetic Beads	Unnecessary	Unnecessary

the frequency shifted when 2 μl of purified water was dropped five times on the IDC by a micropipette are shown in Fig. 9. The frequency shift was 0.702 GHz on average, and we conclude that the water was successfully detected.

Since the dielectric constant of the sample differs between the case where the sample dropped on the IDC contains only water and the case where the sample contains water with biological substances such as CTCs and exosomes, the detection of biological substances is possible by measuring the amount of frequency shift for both over several times. The results of previous measurements and simulations conducted in our laboratory suggest that the amount of frequency shift changes between a drop of water only and a solution containing exosomes and CTCs[6], [12].

Table I shows the comparison to the previous works of CMOS biosensors using LC-VCO. The proposed system can achieve 49.41% chip area reduction compared to the previous works. In order to achieve broadband operation, the proposed circuit utilizes an active inductor with variable inductance value instead of the spiral inductor used in our previous work, which shows that the proposed circuit has a large frequency tunability compared to the previous work.

V. CONCLUSION

In this paper, an active inductor-based VCO with a relatively small chip area and wide bandwidth operation is employed for the detection of CTCs and exosomes. Since the detection principles of the proposed circuits are both based on the dielectric constant of biological materials, magnetic bead labeling is not required for target detection. In addition, the proposed active inductor biosensor can operate over a wide frequency range in γ-dispersion and is expected to detect a wide range of dielectric properties. Using IDC as the capacitance in the detection region, we have demonstrated the feasibility of cell detection on the biosensor chip by electromagnetic field simulation. Furthermore, Post layout simulation was performed using PDK. We confirmed that the amount of frequency shift changes when the equivalent capacitance of the cells dropping on the sensor changes. In the actual measurement using the prototype, water was successfully detected. Therefore, this biosensor has the potential to detect biomarkers such as CTCs and exosomes.

ACKNOWLEDGMENT

This research was financially supported by JST, PRESTO (No. JPMJPR15D5), by Council for Science. Technology and Innovation(CSTI), Cross-ministerial Strategic Innovation Promotion Program (SIP), "Energy systems toward a decarbonized society" (Funding agency: JST), by a Grant-in-Aid for Scientific Research (S) (No. 25220906), Grant-in-Aid for Young Scientists (A) (No. 16H06088) from the Ministry of Education, Culture, Sports, Science and Technology of Japan, and by MIC/SCOPE # 152106004 and # 185106001.

REFERENCES

[1] C. Alix-Panabières and K. Pantel, "Clinical Applications of Circulating Tumor Cells and Circulating Tumor DNA as Liquid Biopsy," *Cancer Discovery*, vol. 6, no. 5. pp. 479–491, 2016.

[2] E. Crowley, F. Di Nicolantonio, F. Loupakis, and A. Bardelli, "Liquid biopsy: monitoring cancer-genetics in the blood," *Nature Reviews Clinical Oncology*, vol. 10, no. 8. pp. 472–484, 2013.

[3] D. L. Adams *et al.*, "Cytometric characterization of circulating tumor cells captured by microfiltration and their correlation to the CellSearch(®) CTC test," *Cytometry A*, vol. 87, no. 2, pp. 137–144, Feb. 2015.

[4] J.-C. Chien and A. M. Niknejad, "Oscillator-Based Reactance Sensors With Injection Locking for High-Throughput Flow Cytometry Using Microwave Dielectric Spectroscopy," *IEEE J. Solid-State Circuits*, vol. 51, no. 2, pp. 457–472, Feb. 2016.

[5] C. Sideris, P. P. Khial, and A. Hajimiri, "Design and Implementation of Reference-Free Drift-Cancelling CMOS Magnetic Sensors for Biosensing Applications," *IEEE J. Solid-State Circuits*, vol. 53, no. 11, pp. 3065–3075, Nov. 2018.

[6] S. Murakami, T. Nakanishi, A. Kobayashi, M. Z. Islam, and K. Niitsu, "LC-Voltage-Controlled-Oscillator-Based Biosensor in 180-nm CMOS Process Targeting β-Dispersion for Detecting Exosomes," *2019 IEEE Asia Pacific Conference on Circuits and Systems (APCCAS)*. 2019.

[7] G. Martinsen, S. Grimnes, and H. Schwan, "INTERFACE PHENOMENA AND DIELECTRIC PROPERTIES OF BIOLOGICAL TISSUE," 2002.

[8] G. Schwarz, "A THEORY OF THE LOW-FREQUENCY DIELECTRIC DISPERSION OF COLLOIDAL PARTICLES IN ELECTROLYTE SOLUTION1,2," *J. Phys. Chem.*, vol. 66, no. 12, pp. 2636–2642, Dec. 1962.

[9] L.-H. Lu, H.-H. Hsieh, and Y.-T. Liao, "A Wide Tuning-Range CMOS VCO With a Differential Tunable Active Inductor," *IEEE Transactions on Microwave Theory and Techniques*, vol. 54, no. 9. pp. 3462–3468, 2006.

[10] X. Bao *et al.*, "Modeling of Coplanar Interdigital Capacitor for Microwave Microfluidic Application," *IEEE Transactions on Microwave Theory and Techniques*, vol. 67, no. 7. pp. 2674–2683, 2019.

[11] X. Ma, X. Du, H. Li, X. Cheng, and J. C. M. Hwang, "Ultra-Wideband Impedance Spectroscopy of a Live Biological Cell," *IEEE Transactions on Microwave Theory and Techniques*, vol. 66, no. 8. pp. 3690–3696, 2018.

[12] T. Nakanishi, M. Matsunaga, A. Kobayashi, K. Nakazato, and K. Niitsu, "A 40-GHz fully integrated circulating tumor cell analysis vector network analyzer in 65-nm CMOS technology with coplanar-line-based detection area," Jpn. J. Appl. Phys., vol. 57, no. 3S2, Jan. 2018, Art. no. 03EC01.